



Utilization of micro encapsulated phase change material in asphalt concrete for improving low-temperature properties and delaying black ice

Tam Minh Phan^a, Dae-Wook Park^{b,*}, Hal-Su Kim^c

^a Dept. of Civil Engineering, Kunsan National University, Gunsan-si 54150, Jeollabuk-do, South Korea

^b Dept. of Civil Engineering, Kunsan National University, Gunsan-si 54150, Jeollabuk-do, South Korea

^c GAWOO IND. Co., LTD., South Korea

ARTICLE INFO

Keywords:

Asphalt mixture
Micro encapsulated PCM
Cracking resistance
Temperature regulation
Delaying black ice

ABSTRACT

Once black ice happens, it strongly reduces the friction of the tire-road surface, resulting in dangerous driving and reducing the performance of asphalt mixture. This study aims to utilize latent heat fusion during phase transition of micro encapsulated phase change material (μ PCM) to improve low-temperature performances and delay black ice formation. The properties of asphalt mixture were carried out by several laboratory experiments. Asphalt slabs with μ PCM additives were exposed to outdoor winter environment to evaluate the effect of μ PCM on temperature regulation. Furthermore, a comparison was studied between fresh and 6-month-old μ PCM slabs to investigate the effectivity of μ PCM latent heat release. Indirect tensile asphalt cracking results showed that containing 1.5% μ PCM (weight of mixture) could increase cracking tolerance index and indirect tensile strength at low temperature (4 °C). Fatigue loading test concluded that all μ PCM modified asphalt mixtures are within normally accepted performance, while monotonic loading test indicated that the addition of an appropriate μ PCM could improve reflection cracking resistance at low temperature. The presence of μ PCM could mitigate low temperature cracking damage by decreasing stiffness and increasing phase angle of asphalt mixture. Besides, the monitored temperature showed that μ PCM modified mixture acquired 2 °C higher compared to conventional mixture. The delay freezing was approximately 1 h and 10 min, which may benefit in delay black ice formation. After six months exposed to outdoor conditions, the latent heat fusion of μ PCM was still present. Finally, the utilization of μ PCM is a promising solution to improve low temperature cracking resistance and delaying black ice formation.

1. Introduction

Over ninety-four percent of paved roads in the United State are surfaced by asphalt concrete [1]. Asphalt concrete pavement is widely used because of its advantages such as construction time, safety, and smoothness. Apart from traffic load, pavement surfaces are directly exposed to the environment throughout its service life [2]. In the summer, asphalt concrete pavements are exposed to hot temperature, resulting to rutting and aging. In contrast, cold temperature climate degrades the quality of asphalt concrete by contraction. This is because asphalt binder is a temperature sensitive material, it soften and stiffens at high and low temperature, respectively [3]. Besides snow during the winter, one extreme problem faced by asphalt pavements is the formation of black ice. Black ice, or commonly called as clear ice, is the formation of glazed ice on the road surface. Once black ice forms, it is very

hard to recognize and strongly reduces friction at tire-road surface thus resulting to car accidents. Based on the annual report from Department of Transportation, over 150,000 automobile crashes are caused by icy pavement [4]. Although there have been several studies on snow-ice melting, there have been limitations. To mention a few examples, the use of road-salt contributes to the corrosion of automobiles and damages pavement structure [5], while using gas-fired or electric boiler causes immense greenhouse effect [6]. In the finding an innovative solution, many researchers have been used phase change materials to regulate the temperature of asphalt concrete pavements [7–9].

Phase change materials have shown to be excellent material for regulating temperature of asphalt mixture to mitigate low temperature distresses [7,10,11]. During transition process, phase change material releases latent heat that increases temperature of the surrounding environment [8]. These materials have been widely used in various

* Corresponding author.

E-mail addresses: dpark@kunsan.ac.kr (D.-W. Park), halsu.kim@gawooind.co.kr (H.-S. Kim).

<https://doi.org/10.1016/j.conbuildmat.2022.127262>

Received 12 August 2021; Received in revised form 26 January 2022; Accepted 21 March 2022

Available online 24 March 2022

0950-0618/© 2022 Elsevier Ltd. All rights reserved.

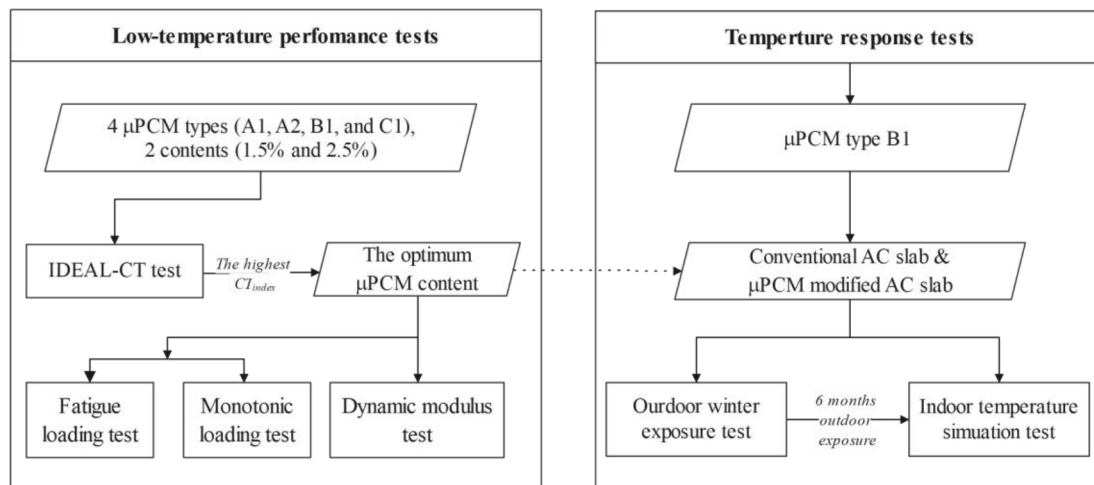


Fig. 1. Research flowchart.

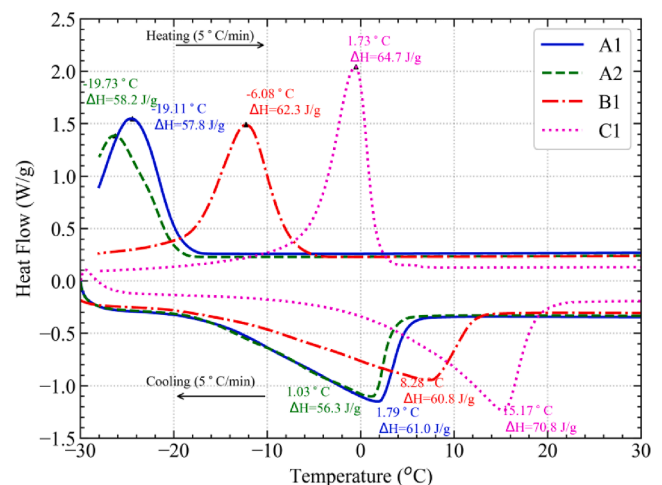
studies for instances thermal energy storage [12], cooling building [7], and solar hot water system [13]. However, direct incorporation of phase change material into asphalt mixture is constrained due to leakage. To properly make use of the phase change material, micro encapsulation has been introduced. The final product, micro encapsulated phase change materials (μ PCM) has proven its advantages such as high heat-storage density, small volume, and good chemical stability [14]. In the previous study, μ PCMs had successfully synthesized with key properties including diameter ranging from 1 to 7 μm , and high thermal stability (95% residual weight at 160 $^{\circ}\text{C}$) [15]. Several studies have also developed μ PCM in asphalt mixture in order to prevent a series of high temperature problems such as aging, fatigue, upheaval, and rutting [9,14,16]. In contrast, only a few research have been developed to mitigate the negative effect of low temperature. The study from Manning et. al., showed that μ PCM modified asphalt mixture could mitigate the effect of frozen process [17]. However, there is still lack of studies on using μ PCMs in enhancing low-temperature properties and delaying black ice formation.

The current study aims to use micro encapsulated phase change material to investigate asphalt mixture's performance at low temperature as well as the ability to delay black ice formation through latent heat release. Four kinds of μ PCM with different transition phrases were examined. Two μ PCM dosages, including 1.5% and 2.5% by weight of mixture were accounted to find the optimum μ PCM content by indirect tensile cracking test (IDEAL-CT). Afterward, fatigue loading test, monotonic loading test, and dynamic modulus test were employed to evaluate asphalt mixture's performance at low temperature. Moreover, two temperature response tests were conducted to validate the effect of μ PCM AC mixture on latent heat release. The first temperature response test was an outdoor winter environment exposure, wherein thermocouples were embedded at various location on an asphalt slab to determine temperature response. The second temperature response test was an indoor temperature simulation, wherein fresh and 6-month-old μ PCM slabs were compared on alternating temperatures to investigate the effectivity of μ PCM latent heat release. The research flowchart of this study is displayed in Fig. 1.

2. Materials – Sample preparation

2.1. Micro encapsulated phase change materials

In the previous study by the authors, micro phase change materials (μ PCMs) had successfully synthesized with a desired transition temperature and latent heat capacity [15]. The μ PCMs were made from n-Tetradecane and silica in certain proportions. The Tween 80 and Span

Fig. 2. Transition phase properties of μ PCMs.

80 were used as surfactants. Synthesized μ PCMs had a perfect sphere with diameter ranging from 1 to 7 μm . The thermal stability (residual weight) was higher than 95% at 160 $^{\circ}\text{C}$ [15]. In current study, to evaluate the effect of phase change temperature on performances at low temperature, four kinds of μ PCMs were investigated. The incorporation of different phase change μ PCM types in this research is expected to further evaluate the impact of transition phase on the performances of asphalt at low temperature. The transition phrases of the μ PCMs are shown in Fig. 2. The A1 and A2 μ PCM has phase change temperature of 1.03 $^{\circ}\text{C}$ and 1.79 $^{\circ}\text{C}$, respectively. Meanwhile, the B1 and C1 has transition phase at 8.28 $^{\circ}\text{C}$ and 15.17 $^{\circ}\text{C}$, respectively. The enthalpy of all four μ PCMs ranges from 56 to 72 J/g.

2.2. Preparation of asphalt mixture

The asphalt mixture is used to investigate the effect of μ PCMs has a nominal maximum aggregate size of 13 mm (AC-13). The coarse, fine, and filler aggregate were made from limestone. The aggregate gradation is shown in Table 1. The PG 64-22 asphalt binder was used in this study. This binder has penetration of 70 (25 $^{\circ}\text{C}$, 0.1 mm), melting point of 48 $^{\circ}\text{C}$, and a density of 1.02 g/cm^3 . The optimum asphalt content was 5.4% by weight of total mixtures. In this research, μ PCMs are considered as a modifier agent, which is directly added into asphalt mixture. Therefore, the filler was not substituted by μ PCMs [10].

Prior to mixing, aggregates and asphalt binder were heated in an

Table 1
Aggregate gradation.

Sieve size (mm)	19	12.5	9.5	4.75	2.36	0.6	0.3	0.15	0.075
Percent passing (%)	100	98	86	60	45	23	14	8	3

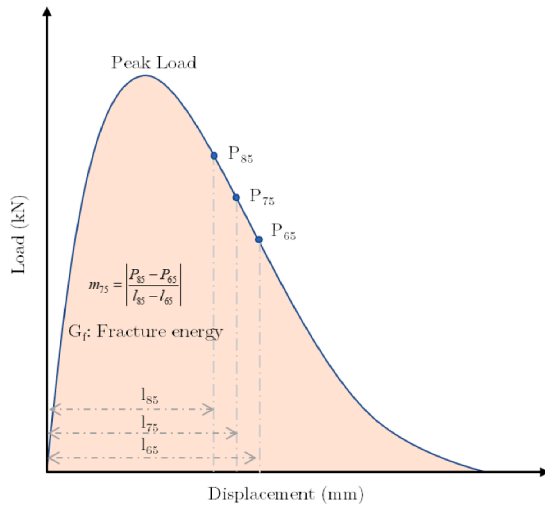


Fig. 3. Load-displacement curve.

oven at 160 °C for 4 h. Mixing process can be referenced from the following steps. First, the aggregates and μ PCMs were mixed at low speed of 60 RPM (rotation per minute) for one minute, then adding asphalt binder and they were continually mixed at 120 RPM for two minutes [18]. Second, the asphalt mixture was conditioned at 140 °C for two hours before compaction to mimic the production and transportation process. The samples for low-temperature performance tests were compacted by Super Gyration Compactor (SGC) with the designed air void of $7 \pm 1\%$. Meanwhile, the samples for temperature response tests were compacted by way of a mini vibratory plate compactor with a desired height to control air void of $7 \pm 1\%$.

3. Test methods

3.1. Performance of μ PCM modified asphalt mixture

3.1.1. Indirect tensile asphalt cracking test (IDEAL-CT)

The cracking resistance of asphalt mixture was investigated by indirect tensile asphalt cracking test (IDEAL-CT). Two dosages of μ PCM were accounted, including 1.5% and 2.5% by weight of the total mixture to find the optimum μ PCM content. A cylindrical sample was compacted using SGC with a size of 150 mm in diameter, and 62.5 mm in height. The air void of sample was controlled at $7 \pm 1\%$. At least three samples per mixture were prepared. The testing temperature of 4 °C was chosen to evaluate the effect of μ PCM on properties of asphalt mixture at low temperature. Dynamic Testing System 30 kN (DTS-30) machine was employed to conduct the IDEAL-CT. To assure uniform temperature on sample specimens, conditioning was conducted in a low-temperature incubator for two hours. A vertical force was applied across the specimen's diameter with a constant loading rate of 50 mm/min. During testing, load and displacement were monitored and recorded. Based on the research of Fujie et al., cracking tolerance index (CT_{index}) was calculated to evaluate the cracking resistance [19]. The higher the CT_{index} indicated the better in cracking resistance of asphalt mixture [20,21]. The load–displacement graph was used to computed CT_{index} , as shown in equation (1).

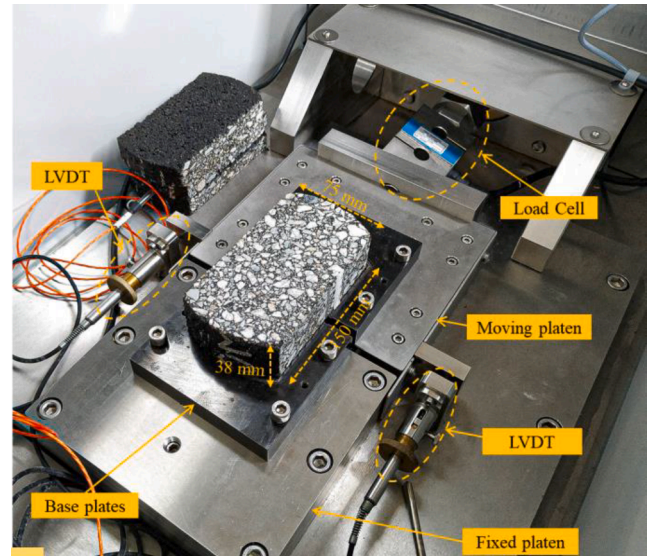


Fig. 4. Test set up of overlay test.

$$CT_{index} = \frac{G_f}{|m_{75}|} \times \left(\frac{l_{75}}{D} \right) \quad (1)$$

where G_f is fracture energy (J/mm^2); is slope at 75% post-peak load, P_x is load $x\%$ of post peak load (N), l_x is displacement at $x\%$ of post peak load (mm) as shown in Fig. 3. In addition, the indirect tensile strength (ITS) was also considered. The ITS is calculated following equation (2).

$$ITS = \frac{2P}{\pi Dt} \quad (2)$$

where P is the peak load (N), and t is thickness of sample (mm).

3.1.2. Fatigue loading test

The fatigue cracking resistance potential of asphalt mixture was evaluated by using an overlay tester (OT) machine. The OT simulates the propagation of fatigue or reflective cracking in the laboratory [22]. An OT cycle consisted of 5 s of loading and 5 s unloading. The test was performed under control strain of 0.63 mm/min and loading rate of 0.1 Hz. According to test specification Tex-248-F, the test was terminated when reaching 93% reduction in the initial peak load [23]. In this test, the crack resistance potential of asphalt mixture was considered as the number of load cycles until test termination. For OT specimen preparation, a 150 mm cylindrical sample was compacted by SGC to achieve air void of $7 \pm 1\%$. Secondly, this sample was trimmed to a specimen with 150 mm in length, 75 mm in width, and 38 mm in height (see Fig. 4). At least three specimens were prepared for each mixture. To glue a sample onto the OT plate, a two-part epoxy with adhesive shear strength of 1500 psi was used. After gluing, the samples were cured at room temperature for 24 h.

The fatigue loading test was examined at 24 ± 1 °C [24]. Moreover, samples were preconditioned in a temperature incubator at testing temperature for two hours before testing. In addition, the Tukey-Kramer (T-K) statistical analysis was employed to compare between different asphalt mixtures. The T-K value is based on calculating confidence interval for the difference between each pair of averages (μ). This

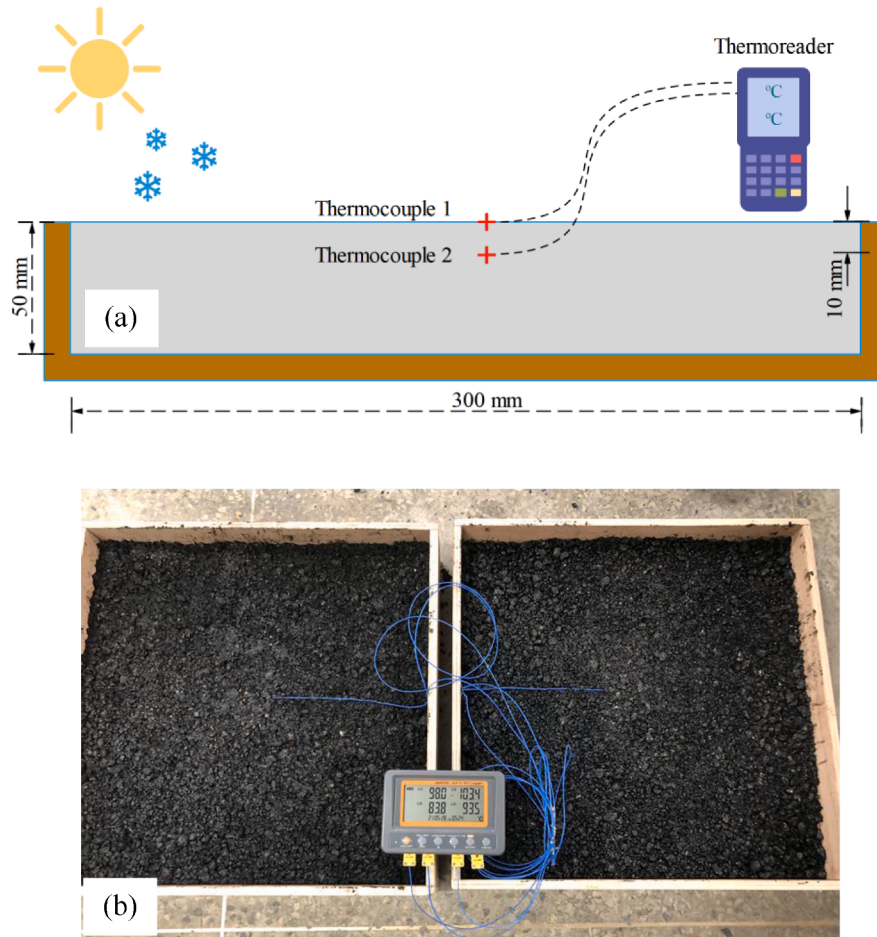


Fig. 5. (a) Embedment diagram of thermocouples and (b) Preparation of two slabs.

statistical tool will present whether each asphalt mixture is significantly different or not [25].

3.1.3. Monotonic loading test

The monotonic loading test follows the same specimen preparation with fatigue loading test samples. It was conducted at $4 \pm 1 \text{ }^\circ\text{C}$ and was performed under displacement-controlled setting. It had a displacement rate of 3.375 mm/min with a maximum displacement of 3.375 mm. Monotonic loading was terminated when sample reached 99% reduction of peak load. The primary output from R-OT is the load–displacement curve that is used to calculate critical fracture energy index (CEI) and material tensile strength [26]. The CEI is defined as the area under the load–displacement curve, while the material strength is defined as the peak load divided by the cross sectional area as shown in equation (33). Where, P_{max} is maximum load (N), t is sample thickness (mm), and w is sample width (mm).

$$\sigma_t = \frac{P_{max}}{t \times w} \quad (3)$$

3.1.4. Dynamic modulus test

In this study, dynamic modulus test was carried out by DTS-30 machine. The 150 mm cylindrical samples were compacted by SGC to achieve $7 \pm 1 \%$ of air void. After cutting and coring, three cylindrical samples (100 mm in diameter, 150 in height) were prepared for each mixture According to AASHTO TP T342-11, at least three test temperatures were selected, including $4 \text{ }^\circ\text{C}$, $21 \text{ }^\circ\text{C}$, and $37 \text{ }^\circ\text{C}$ [27]. The samples were preconditioned at certain temperature for three hours to obtain

uniform temperature distribution. For each testing temperature, six loading frequencies were applied from the highest to the lowest (e.g., 25, 10, 5, 1, 0.5, and 0.1 Hz). An axial compressive stress was then imposed on samples to obtain axial strains between 50 and 150 microstrains. The dynamic modulus ($|E^*|$) is calculated by Eq. (4). Where, σ_0 is the applied stress amplitude (MPa), while ϵ_0 is the measured strain amplitude. Furthermore, phase angle is defined as the angle in degrees to which resulting peak strain lags behind the sinusoidal applied peak stress. The phase angle is calculated by equation (5) wherein, f is frequency (Hz), and Δt is lag time (s) between stress and strain [2].

$$|E^*| = \frac{\sigma_0}{\epsilon_0} \quad (4)$$

$$\varphi = 2\pi f \Delta t \quad (5)$$

Dynamic modulus master curves and phase angle master curves were constructed by principle of time–temperature superposition as expressed in Eqs. (6) and (7) [28]. The reference temperature of $21 \text{ }^\circ\text{C}$ was chosen to generate master curves. A shift factor (a_T) is used to generate a smooth master curve, wherein a_T is calculated by Williams-Landel-Ferry (WLF) relation as displayed in Eq. (8) [29]. Where, E_f^* , φ_f is dynamic modulus and phase angle at frequency, respectively; f is loading frequency (Hz); δ , α , λ , β , γ is fitting parameters; α_T is time–temperature shift factor; T is test temperature ($^\circ\text{C}$); T_r is reference temperature ($^\circ\text{C}$); C_1 , C_2 is fitting parameters. Python programming language using SciPy library was employed to find the fitting parameters [30].

$$\log|E_f^*| = \delta + \frac{\alpha}{1 + e^{\beta + \gamma \times \log(f \times a_T)}} \quad (6)$$



Fig. 6. (a) Outdoor temperature test set up, (b) temperature recording on snow day.

$$\varphi_f = -\frac{\frac{\pi}{2} \times \alpha \times \gamma \times e^{\beta + \gamma \times \log(f \times a_T)}}{[1 + \lambda \times e^{\beta + \gamma \times \log(f \times a_T)}]^{1 + \frac{1}{n}}} \quad (7)$$

$$\log a_T = -\frac{C_1 \times (T - T_r)}{C_2 + (T - T_r)} \quad (8)$$

3.2. Temperature response of μPCM modified asphalt mixture

3.2.1. Outdoor temperature response test

This test aims to evaluate the effect of phase change material on the temperature response of asphalt mixture under outside winter conditions. The μPCM mixture with the highest cracking tolerance index from IDEAL-CT was chosen for this test with a control sample. Two asphalt mixture slabs were prepared, including control slab (without μPCM) and μPCM slab with a dimension of 30 × 30 × 5 cm. A mini vibratory plate compactor was employed to compact both slabs at a certain thickness to obtain 7 ± 1 % of air void. As displayed in Fig. 5a, two thermocouples were embedded on each slab, one at the surface and the other at 10 mm depth. The thermocouple wire probe type K (TP-01) was used in this study with a precision of 0.1 °C, and a temperature capacity of -40 °C to 250 °C. A four channels thermometer was employed to record the temperature of two slabs by intervals of 10 min. The thermometer has a temperature range of -200 °C to 1370 °C with accuracy of 0.1 °C. Two slabs were preconditioned in laboratory for 48 h. The sample's temperature was recorded to ensure the proper operation of the four thermocouples (Fig. 5b).

To equilibrate drastic changes of temperature from transferring slabs from production area to outdoor environment, a two-day outdoor

exposure was first observed prior to temperature monitoring. Real time temperature responses were monitored (from January 30th to February 6th) with an interval of 10 min as shown in Fig. 6. Throughout the test, weather conditions such as air temperature, wind speed, wind direction, humidity, dew point, and snow precipitation were recorded [31]. To quantify the effect of μPCM on the delay of black ice formation through latent heat release, delay freezing time was developed. Since the formation of black ice is recorded at 0 °C, this study employs a similar concept to phase angle, wherein the time lag between two temperature curve readings taken from control and μPCM slab would define delay freezing time. The delay freezing time is computed by the time difference when both mixtures reach 0 °C temperature readings.

3.2.2. Indoor temperature response test

The indoor test is used to determine the effectual latent heat release of μPCM slab after being exposed to prolonged real time outdoor conditions. The two aged slab mixes were taken from the outdoor temperature response test renamed into CTR-old and PCM-old for control and μPCM mixture, respectively. This study employed a six-month outdoor exposure starting from January 30th to July 1st. In addition, two “new” slabs were prepared following the same procedure as an outdoor temperature response test having dimensions of 50 × 50 × 5 cm, and air void of 7 ± 1 %. Two thermocouples were also embedded into the samples (i.e., at surface and 10 mm below the surface). After preparation, temperature responses were monitored for 48 h to guarantee the precise functioning of the thermocouples.

As shown in Fig. 7a, four slabs were placed in a temperature incubator, including two old slabs (six months exposed to outdoor conditions) and two fresh slabs. Prior to cooling-heating simulation, all slab samples were conditioned at 21 °C at least 12 h to achieve a homogenous

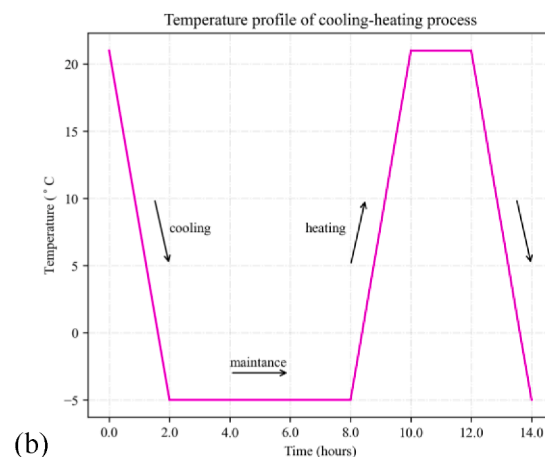
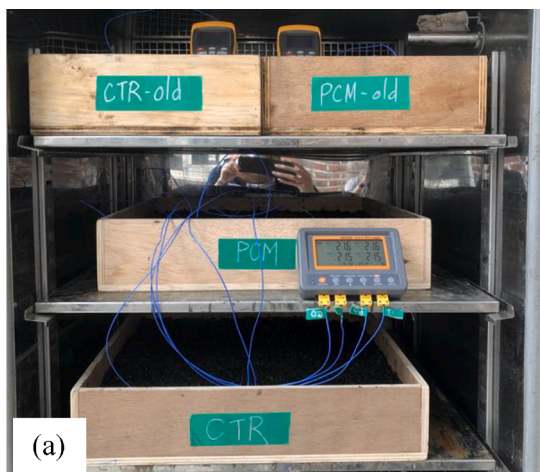


Fig. 7. (a) Indoor temperature test set up, (b) cooling-heating temperature profile.

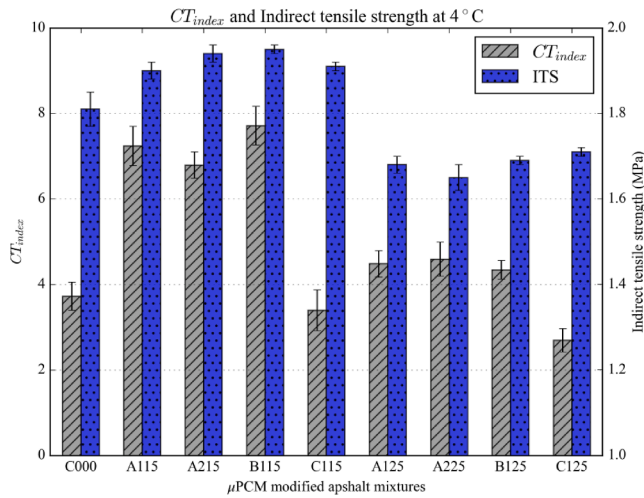


Fig. 8. CT_{index} and indirect tensile strength at 4 °C.

temperature distribution. The cooling-heating process includes the following steps. First, the incubator’s temperature was decreased from 21 °C to −5 °C for two hours and maintained for 6 h (12 h) thereafter. Second, the incubator was heated back to 21 °C for two hours. Lastly, the temperature was reduced to −5 °C at a rate of 13 °C/hr. The cooling-heating temperature simulation can be referenced from Fig. 7b. During the simulation process, the humidity was controlled at 90%. The temperature response of all four asphalt mixture slabs were recorded every minute. The effectivity of μ PCM’s latent heat release was based on the difference between temperature curve readings of fresh and 6-month old slabs.

4. Results – Discussions

4.1. Performance tests

4.1.1. IDEAL-CT

Fig. 8 shows the cracking tolerance index (CT_{index}) at 4 °C. It was found that asphalt mixtures containing 1.5% μ PCM increased the CT_{index}

substantially compared to others. Among four kinds of μ PCM, the B1 mixture gained the highest value and followed by A1 and A2 mixture, which were 7.88, 7.54, and 7.21, respectively. The higher CT_{index} may be accounted for the transition phase of each μ PCM as depicted in Fig. 2. It is observed that μ PCM with transition phase temperature (i.e., 1.79 °C, 1.03 °C, and 8.28 °C for μ PCM A1, A2, and B1, respectively). Besides, having 2.5% μ PCM modified asphalt mixture showed unexpected results, having lower CT_{index} than that of 1.5% μ PCM content. Although μ PCMs could release latent heat and increase temperature of samples at low temperature, overdosing μ PCM content could increase mineral particles and may deteriorate properties of the asphalt mixture. With 2.5%, the A2 gained the highest CT_{index} (4.29) while the C1 mixture (3.03) was lower than the control sample (3.87). The C1 mixture presented a poor result due to the early transition phase temperature of 15.17 °C. The latent heat release of the μ PCM could have been exhausted upon reaching the test temperature of 4 °C.

The indirect tensile strength (ITS) of asphalt mixture at 4 °C is shown in Fig. 8. The ITS of 1.5% μ PCM mixtures were higher than that of 2.5% and control mixture. The highest ITS belonged to B115, which was 1.91 MPa. Although the CT_{index} of B115 mixture was double that of C000 mixture, the ITS was only 5% higher. This can be explained by comparing both Eqs. (1) and (2). The CT_{index} was calculated based on the fracture energy and the slope at 75% post peak load, while ITS was based only on peak load. A higher CT_{index} describes a ductile behavior of an asphalt mixture, which may come from high fracture energy or prolonged 75% post peak load. As shown in Fig. 9, the load versus displacement of asphalt mixtures with 1.5% μ PCM content clearly depicts ductility compared to control sample. It is obvious from Fig. 9 that load–displacement curves for 2.5% μ PCM content were not much different to the control sample, this may have caused the insignificant increase in CT_{index} . From the test results, the 1.5% μ PCM content has shown significant improvement for low temperature cracking resistance of asphalt mixture; consequently, 1.5% content of type B1 μ PCM by weight of total mixture was chosen for further examination on outdoor and indoor temperature response test.

4.1.2. Fatigue loading test

Fatigue loading test results are displayed in Fig. 10. Since asphalt mixture becomes too brittle under low temperature, 24 °C was selected to conduct the fatigue loading. The numbers of OT cycles were recorded

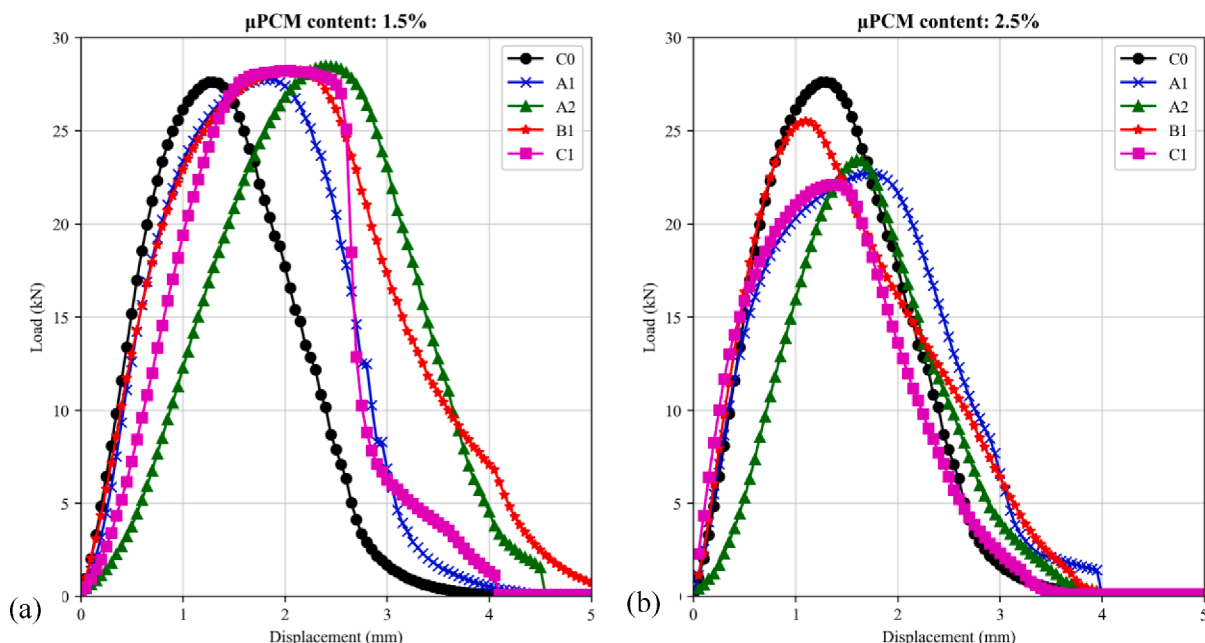


Fig. 9. Load displacement of (a) 1.5% mixtures and (b) 2.5% mixtures.

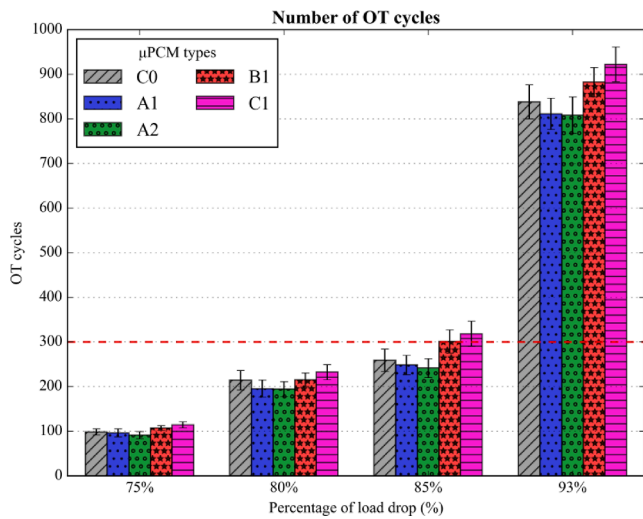


Fig. 10. Number of OT cycles.

Table 2

Tukey-Kramer multiple comparison at 93% reduction of peak load.

Comparison	Lower value	Upper value	Conclusion
C0 to A1	-27.2	47.9	Not significantly different
C0 to A2	-19.9	55.2	Not significantly different
C0 to B1	-4.8	75.9	Not significantly different
C0 to C1	-22.1	77.2	Not significantly different

during fatigue loading test. As portrayed, the C1 mixture achieved the highest OT cycles, which were 323 and 942 cycles at 85% and 93%, respectively. The higher OT cycles indicated better resistance to fatigue or reflection cracking. As shown in Fig. 10, at 75% reduction of peak load, AC mixes obtained only 100 OT cycles on average; moreover, these values were at around 200 cycles at 80% drop of peak load. To validate the mixtures, the research from Collin et al. showed that OT cycles for asphalt mixture should have a minimum of 300 cycles at 93% [32]. It can be concluded that all μPCM modified asphalt mixtures are within minimum accepted performance. To further analyze the effect of μPCMs

on the number of OT cycles, the Tukey-Kramer multiple comparison was employed to find the significant differences among the mixtures. As shown in Table 2, control and other μPCM mixtures were not significantly different. In other words, the addition of μPCM did not deteriorate performance of asphalt mixtures.

4.1.3. Monotonic loading test

The monotonic loading test was employed to find the effect of phase change material (phase change temperature) on reflection cracking at low temperature. Therefore, temperature of 4 °C was chosen to examine monotonic loading test. Due to the brittle of sample at low temperature, the load versus displacement behavior was only recorded at the first OT cycle. Typically, the monotonic loading test was terminated after 10 cycles or 99% reduction of peak load. As displayed in Fig. 11a, A1 mixture gained the most ductile behavior, and followed by A2 and B1 mixture. Furthermore, the critical fracture energy (CEI) was computed as shown in Fig. 11b. In general, the higher the value of CEI represents the greater energy requirement to initiate the first crack. Due to its ductile behavior, A1 mixture acquired the highest CEI, which was 689 J/mm² compared to that of control sample (423 J/mm²). This may be due to the release of latent heat fusion which could reduce the stiffness of asphalt mixture. Moreover, the C1 mixture showed the lowest CEI (389 J/mm²), this phenomenon was consistent with the results obtained from IDEAL-CT test. Due to the high transition phase property of type C1 μPCM (at 15.17 °C), at testing temperature of 4 °C it may have already exhausted its latent heat release capacity. It can be concluded that the addition of an appropriate μPCM could improve the resistance to reflection cracking at low temperature.

4.1.4. Dynamic modulus test

Fig. 12a illustrates the dynamic modulus master curves of asphalt mixtures at 21 °C. Overall, μPCM modified asphalt mixtures obtained a lower dynamic modulus than that of the control mixture. The dynamic modulus increased with increasing frequencies or decreasing temperature. Especially, A1 mixture showed the lowest dynamic modulus among the four μPCM mixtures. The addition of μPCM could decrease stiffness of asphalt mixture at low temperatures or at high frequencies (Fig. 12a). Phase angle master curves are presented in Fig. 12b. At the low frequencies or at high temperature, phase angle of control sample was higher than others. However, when increasing frequencies or decreasing

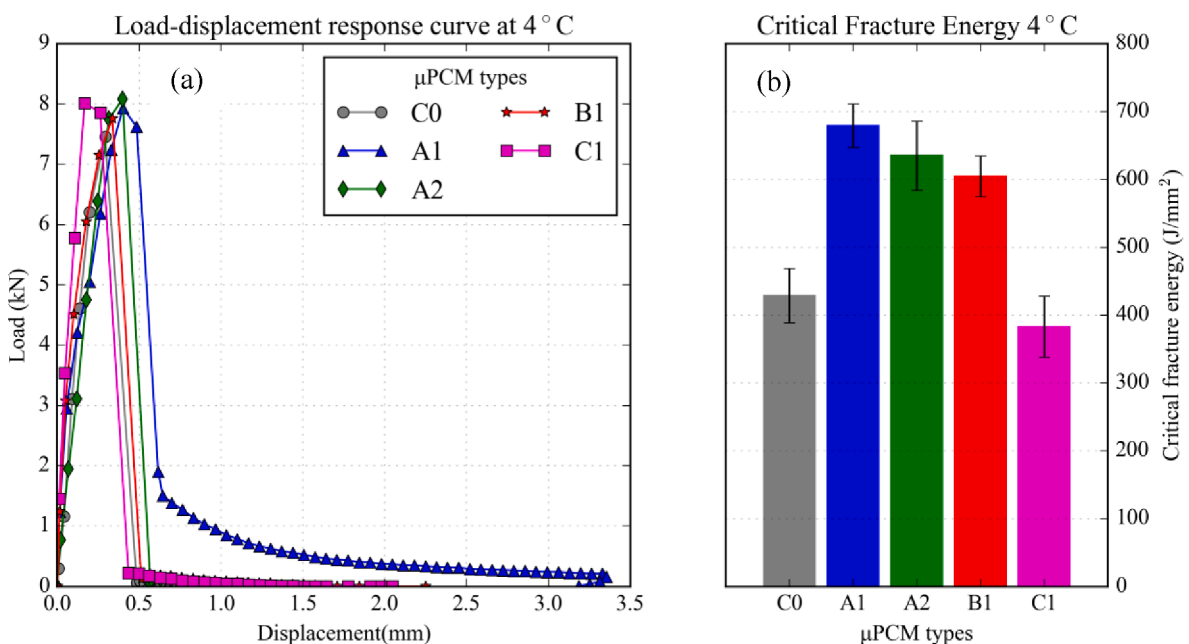


Fig. 11. (a) Load-displacement and (b) Critical fracture energy.

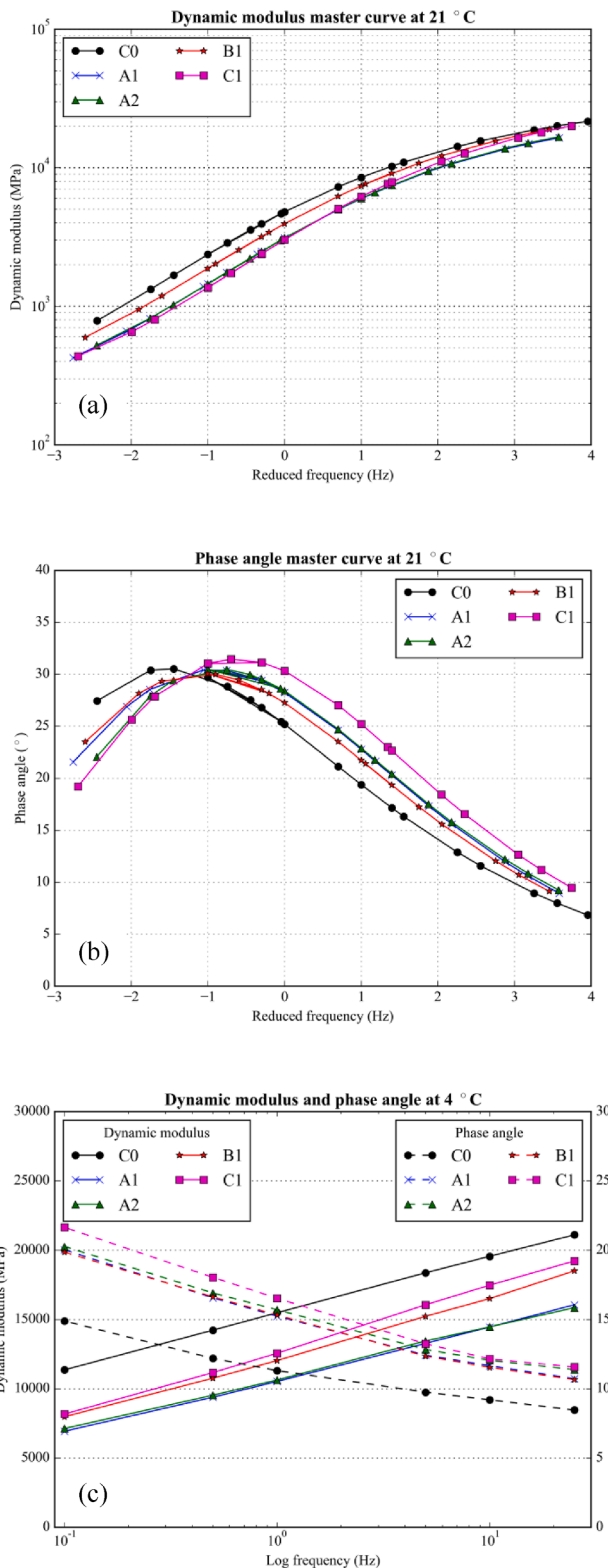


Fig. 12. (a) DM master curve, (b) PA master curve, and (c) test values at 4 °C.

of temperature, the phase angle of μ PCMs modified mixtures were higher than that of control mixture. Noted that phase angle is defined as the time lag between stress and strain behavior. Therefore, the lower the phase angle indicated the better in delaying stress strain behaviors. In other words, mixes containing μ PCMs could improve the resistance to low temperature cracking of asphalt mixture.

To clarify the effect of μ PCMs on dynamic modulus and phase angle

at low temperature, Fig. 12c presents the dynamic modulus at 4 °C with various frequencies. Results showed that dynamic modulus increased with increasing testing frequencies. The dynamic modulus value of control mixture was the highest. Meanwhile, utilization of μ PCMs could reduce dynamic modulus of asphalt mixture at 4 °C especially A1 and A2 mixtures. This may be due to the transition phase property of both μ PCMs having 1–2 °C. In contrast, the phase angles were inversely proportional with the testing frequencies. The control mixture gained the lowest phase angle values compared than all μ PCM mixtures. Finally, the addition of μ PCMs could reduce the stiffness of asphalt mixture and increase phase angle at low temperature (e.g., 4 °C).

4.2. Temperature response tests

4.2.1. Outdoor temperature response test

The temperature responses of two asphalt mixture slabs are shown in Fig. 13. In order to analyze the effect of μ PCM on the delay of black ice formation through latent heat release, two thermocouples were embedded on each concrete slab. Overall, the temperature responses of two slabs showed sinusoidal behavioral changes, which was the effect of environment temperature. From 11:00 AM to 5:00 PM (KST), the average temperatures in the slab were extremely higher compared to the environment temperature. Because of solar radiation, asphalt mixture could absorb solar radiation at the surface. However, during nighttime when air temperature dropped down below 5 °C, it was observed that μ PCM slab would release latent heat that maintained pavement temperature for 2 degrees higher. Therefore, the temperature of μ PCM slab slightly reduced compared to control slab. This phenomenon can be defined as delay freezing time. The μ PCM modified asphalt mixture acquired a delay freezing duration of 1 h and 10 min per day.

The contribution of μ PCM is mainly beneficial during winter season, especially in snow days. As shown in Fig. 14, the snow melting process of μ PCM slab was faster than that of control slab. This may be due to the released latent heat of μ PCM when air temperature decreases. It is interesting to found that the temperature of μ PCM slab was slightly higher than snow temperature (0 °C), which caused early snowfall to melt. Thus, this finding confirmed the effectiveness of μ PCM in the governing of pavement temperature.

4.2.2. Indoor temperature response test

This test aims to determine the effectivity of μ PCM's latent heat fusion release after prolonged exposure to outside conditions. In this testing stage, four asphalt mixture slabs were examined. The temperature responses of slabs are portrayed in Fig. 15. From the figure, both PCM-old and PCM-new clearly showed similarity on their temperature profile. Although, slabs were experienced to 6 h (12 h) at -5 °C, the effect of μ PCM was remained stable. When air temperature decreased to 8 °C, μ PCM released latent that helped regulate temperature of μ PCM slab slightly above 7.8 °C. Both old μ PCM slab and new μ PCM slab presented the effect of μ PCM's latent heat fusion release.

Consider to cooling process, the temperature of PCM-new slab was slightly higher than that of CTR-new slab, which was 1–2 °C higher at phase transition of μ PCM. The delay freezing time was approximately 1 h and 30 min. Meanwhile, the delay freezing time of PCM-old sample was 1 h and 10 min. It can be concluded that after 6 months exposure to outdoor conditions, the effect of μ PCM was preserved.

5. Conclusions

In this research, the effect of μ PCM on low-temperature performances of asphalt mixture and delaying black ice formation through latent heat fusion release were examined. The performances of asphalt mixtures were conducted by IDEAL-CT, repeated loading test, monotonic loading test, and dynamic modulus test. Besides, the temperature responses of μ PCM modified asphalt mixture was examined by outdoor and indoor test. The following key findings were drawn below:

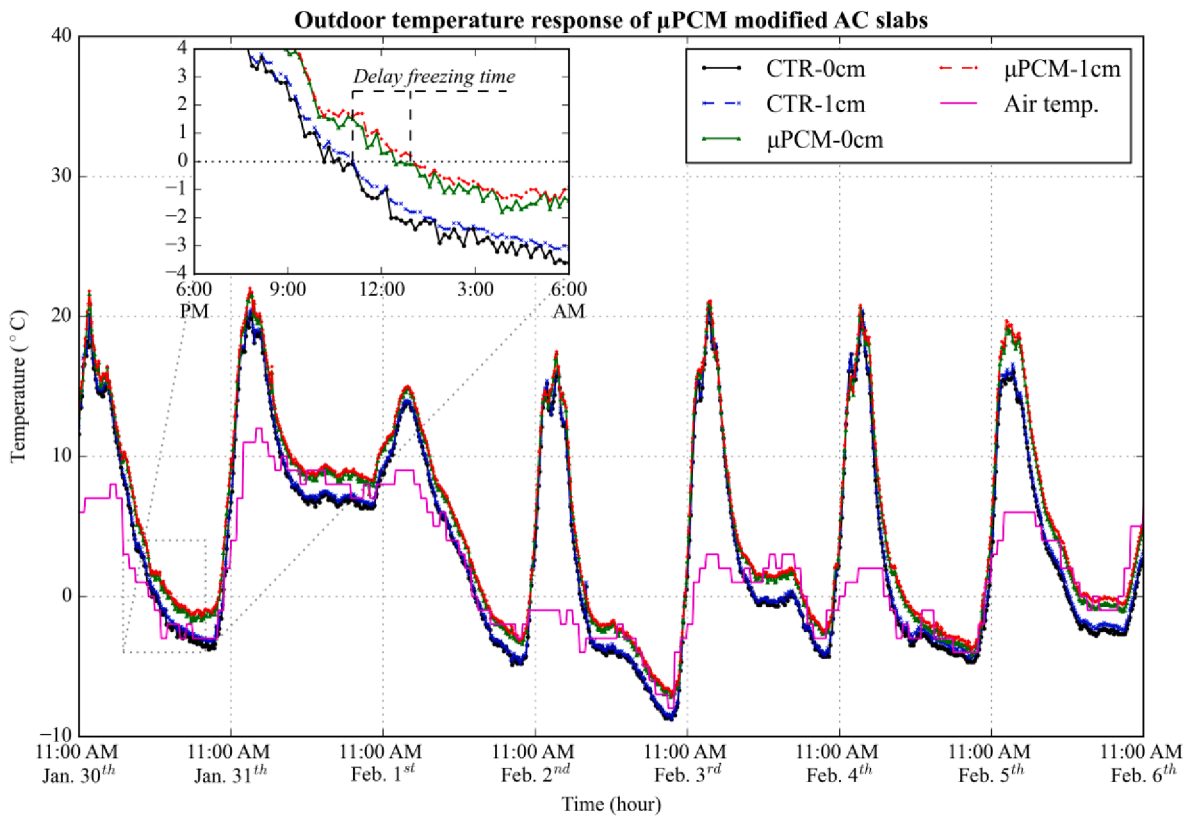


Fig. 13. Outdoor temperature response.

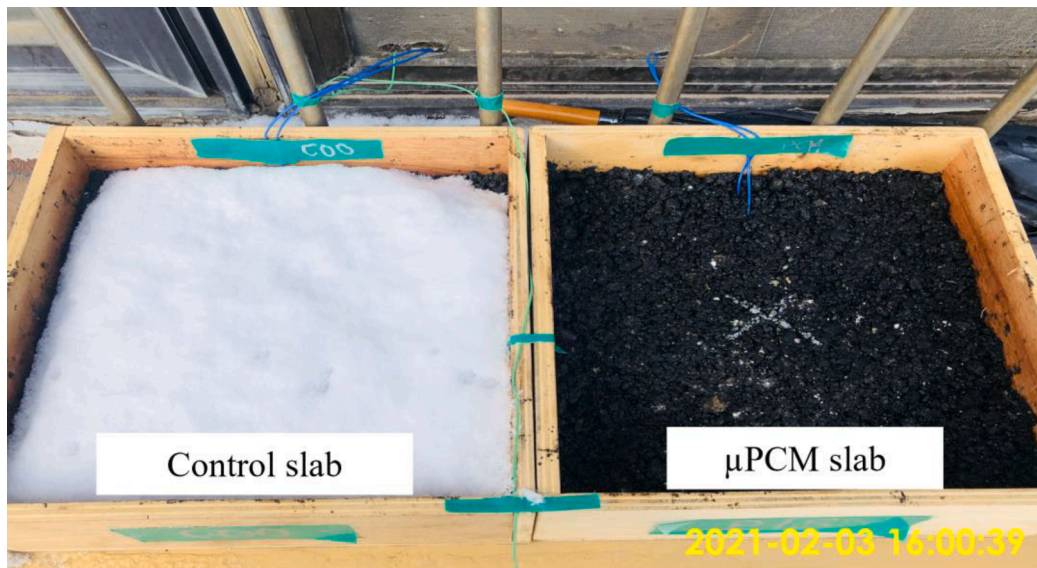


Fig. 14. Snow melting of control slab and μPCM slab.

- An appropriate μPCM with 1.5% (by weight of mixture) helped asphalt mixture gain a higher CT_{index} than that of control sample. Mixtures containing μPCM could improve cracking resistance and enhance indirect tensile at low temperature (e.g., 4 °C). The μPCM type B1 having phase change temperature of improve the ductile behavior of asphalt mixture.
- The results from repeated loading test presented that μPCM modified asphalt mixtures are within normally accepted performance. Meanwhile, monotonic loading test showed that an appropriate usage of μPCM could improve critical fracture energy of asphalt mixture. In

other words, μPCM could enhance resistance to fatigue and reflection cracking at low temperature.

- Modification of μPCM could reduce the stiffness and increase the phase angle of asphalt mixture, which is beneficial in improving low temperature cracking resistance.
- The results from outdoor temperature response test indicated that the μPCM slab gained a 2 °C higher compared to conventional slab. Due to the latent heat fusion of μPCM, delay freezing time was approximately 1 h and 10 min per day.

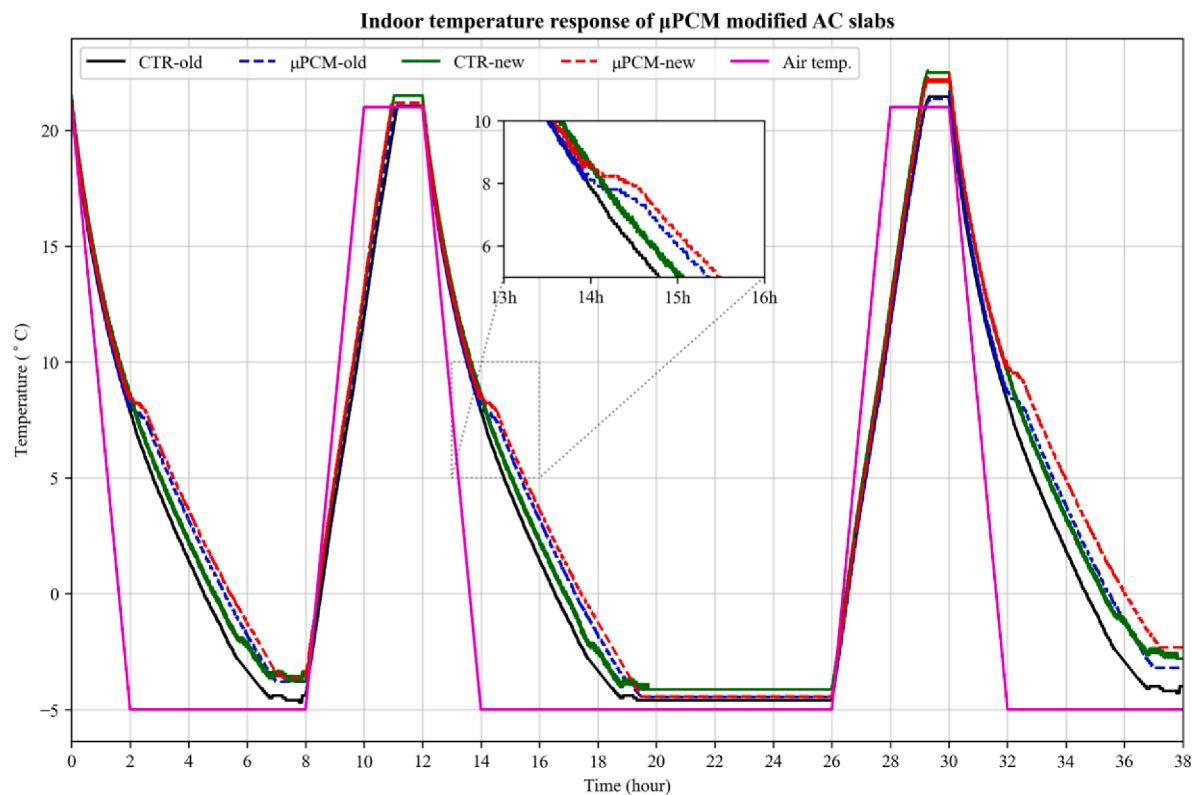


Fig. 15. Indoor temperature response.

- After six months exposure to outdoor conditions, the effect of μ PCM on temperature regulation was preserved. Therefore, μ PCM is promising solution to delay black ice formation through latent heat fusion.

CRediT authorship contribution statement

Tam Minh Phan: Methodology, Software, Validation, Data curation, Writing – original draft, Writing – review & editing. **Dae-Wook Park:** Conceptualization, Methodology, Validation, Data curation, Writing – review & editing. **Hal-Su Kim:** Validation, Data curation, Writing – review & editing.

Declaration of Competing Interest

The authors declare that they have no known competing financial interests or personal relationships that could have appeared to influence the work reported in this paper.

Acknowledgements

This research was supported by a grant from Infrastructure and Transportation Technology Promotion Research Program funded by the Ministry of Land, Infrastructure and Transport of Korean Government (Code 20CTAP-C157548-01).

References

- [1] National Asphalt Pavement Association, The Asphalt Pavement Industry Fast Facts, Natl. Asph. Pavement Assos. (n.d.). <https://www.asphaltpavement.org>.
- [2] T.W.K. E. Ray Brown, Prithvi S. Kandhal, Freddy L. Roberts, Y. Richard Kim, Dah-Yinn Lee, Hot mix asphalt materials, mixture design, and construction, 2009.
- [3] T.M. Phan, D.-W. Park, T.H.M. Le, Crack healing performance of hot mix asphalt containing steel slag by microwaves heating, *Constr. Build. Mater.* 180 (2018) 503–511, <https://doi.org/10.1016/j.conbuildmat.2018.05.278>.
- [4] D. of Transportation, How Do Weather Events Impact Roads?, (n.d.). https://ops.fhwa.dot.gov/weather/q1_roadimpact.htm.
- [5] E.S. Rødland, E.D. Okoffo, C. Rauert, L.S. Heier, O.C. Lind, M. Reid, K.V. Thomas, S. Meland, Road de-icing salt: assessment of a potential new source and pathway of microplastics particles from roads, *Sci. Total Environ.* 738 (2020), 139352, <https://doi.org/10.1016/j.scitotenv.2020.139352>.
- [6] K. Mensah, J.M. Choi, Review of technologies for snow melting systems, *J. Mech. Sci. Technol.* 29 (2015) 5507–5521, <https://doi.org/10.1007/s12206-015-1152-4>.
- [7] F. Souayfane, F. Fardoun, P.-H. Biwolé, Phase change materials (PCM) for cooling applications in buildings: a review, *Energy Build.* 129 (2016) 396–431, <https://doi.org/10.1016/j.enbuild.2016.04.006>.
- [8] M. Bueno, M.R. Kakar, Z. Refaa, J. Worlitschek, A. Stamatou, M.N. Partl, Modification of asphalt mixtures for cold regions using microencapsulated phase change materials, *Sci. Rep.* 9 (2019) 20342, <https://doi.org/10.1038/s41598-019-56808-x>.
- [9] D. Yinfei, L. Pusheng, W. Jiacheng, D. Hancheng, W. Hao, L. Yingtao, Effect of lightweight aggregate gradation on latent heat storage capacity of asphalt mixture for cooling asphalt pavement, *Constr. Build. Mater.* 250 (2020), 118849, <https://doi.org/10.1016/j.conbuildmat.2020.118849>.
- [10] B. Ma, S. Chen, K. Wei, F. Liu, X. Zhou, Analysis of thermoregulation indices on microencapsulated phase change materials for asphalt pavement, *Constr. Build. Mater.* 208 (2019) 402–412, <https://doi.org/10.1016/j.conbuildmat.2019.03.014>.
- [11] X. Zhou, G. Kastiukas, C. Lantieri, P. Tataranni, R. Vaiana, C. Sangiorgi, Mechanical and thermal performance of macro-encapsulated phase change materials for pavement application, *Materials* 11 (8) (2018) 1398, <https://doi.org/10.3390/ma11081398>.
- [12] M.J. Santamouris, C.C. Lefas, On the coupling of PCM stores to active solar systems, *Int. J. Energy Res.* 12 (1988) 603–610, <https://doi.org/10.1002/er.4440120404>.
- [13] C. Solé, M. Medrano, A. Castell, M. Nogués, H. Mehling, L.F. Cabeza, Energetic and exergetic analysis of a domestic water tank with phase change material, *Int. J. Energy Res.* 32 (2008) 204–214, <https://doi.org/10.1002/er.1341>.
- [14] K. Wei, B. Ma, X. Huang, Y. Xiao, H. Liu, Influence of NiTi alloy phase change heat-storage particles on thermophysical parameters, phase change heat-storage thermoregulation effect, and pavement performance of asphalt mixture, *Renew. Energy* 141 (2019) 431–443, <https://doi.org/10.1016/j.renene.2019.04.026>.
- [15] T. Minh Phan, D.-W. Park, T. Ho Minh Le, Improvement on rheological property of asphalt binder using synthesized micro-encapsulation phase change material, *Constr. Build. Mater.* 287 (2021) 123021, <https://doi.org/https://doi.org/10.1016/j.conbuildmat.2021.123021>.
- [16] Y. Chen, H. Wang, Z. You, N. Hossiney, Application of phase change material in asphalt mixture – A review, *Constr. Build. Mater.* 263 (2020), 120219, <https://doi.org/10.1016/j.conbuildmat.2020.120219>.

- [17] B.J. Manning, P.R. Bender, S.A. Cote, R.A. Lewis, A.R. Sakulich, R.B. Mallick, Assessing the feasibility of incorporating phase change material in hot mix asphalt, *Sustain. Cities Soc.* 19 (2015) 11–16, <https://doi.org/10.1016/j.scs.2015.06.005>.
- [18] B. Ma, S. Chen, Y. Ren, X. Zhou, The thermoregulation effect of microencapsulated phase-change materials in an asphalt mixture, *Constr. Build. Mater.* 231 (2020), 117186, <https://doi.org/10.1016/j.conbuildmat.2019.117186>.
- [19] F. Zhou, S. Im, L. Sun, T. Scullion, Development of an IDEAL cracking test for asphalt mix design and QC/QA, *Road Mater. Pavement Des.* 18 (2017) 405–427, <https://doi.org/10.1080/14680629.2017.1389082>.
- [20] S.-H. Lee, A.B. Tam, J. Kim, D.-W. Park, Evaluation of rejuvenators based on the healing and mechanistic performance of recycled asphalt mixture, *Constr. Build. Mater.* 220 (2019) 628–636, <https://doi.org/10.1016/j.conbuildmat.2019.05.150>.
- [21] T.M. Phan, S.N. Nguyen, C.-B. Seo, D.-W. Park, Effect of treated fibers on performance of asphalt mixture, *Constr. Build. Mater.* 274 (2021), 122051, <https://doi.org/10.1016/j.conbuildmat.2020.122051>.
- [22] A.B. Tam, D.-W. Park, T.H.M. Le, J.-S. Kim, Evaluation on fatigue cracking resistance of fiber grid reinforced asphalt concrete with reflection cracking rate computation, *Constr. Build. Mater.* 239 (2020), 117873, <https://doi.org/10.1016/j.conbuildmat.2019.117873>.
- [23] Tex-248-F, Test procedure for Overlay Test, (2019).
- [24] J. Li, J. Oh, B. Naik, G.S. Simate, L.F. Walubita, Laboratory characterization of cracking-resistance potential of asphalt mixes using overlay tester, *Constr. Build. Mater.* 70 (2014) 130–140, <https://doi.org/10.1016/j.conbuildmat.2014.07.069>.
- [25] R.L.M.R.F.G.J.L. Hess, *Statistical Design and Analysis of Experiments: With Applications to Engineering and Science*, Second Edition, 2003.
- [26] L.F. Walubita, L. Fuentes, S.I. Lee, O. Guerrero, E. Mahmoud, B. Naik, G.S. Simate, Correlations and preliminary validation of the laboratory monotonic overlay test (OT) data to reflective cracking performance of in-service field highway sections, *Constr. Build. Mater.* 267 (2021) 121029, <https://doi.org/https://doi.org/10.1016/j.conbuildmat.2020.121029>.
- [27] AASHTO-T342-11, Standard Method of Test for Determining Dynamic Modulus of Hot-Mix Asphalt Concrete Mixtures, (2019).
- [28] H. Liu, R. Luo, Development of master curve models complying with linear viscoelastic theory for complex moduli of asphalt mixtures with improved accuracy, *Constr. Build. Mater.* 152 (2017) 259–268, <https://doi.org/10.1016/j.conbuildmat.2017.06.143>.
- [29] M.L. Williams, R.F. Landel, J.D. Ferry, The Temperature Dependence of Relaxation Mechanisms in Amorphous Polymers and Other Glass-forming Liquids, *J. Am. Chem. Soc.* 77 (1955) 3701–3707, <https://doi.org/10.1021/ja01619a008>.
- [30] Python, PYTHON, (2021). <https://www.python.org/>.
- [31] Weather Underground, (n.d.). <https://www.wunderground.com/>.
- [32] J.G. Collin, T.C. Kinney, X. Fu, Full scale highway load test of flexible pavement systems with geogrid reinforced base courses, *Geosynth. Int.* 3 (4) (1996) 537–549.